Study on Sustainable Development of Carbonate Reservoir Based on 3D Printing Technology

Xu Chen[1,2], Zubo Zhang[1,2], Jian Gao[1,2] and Hao Kang[3,*]

[1]*State Key Laboratory of Enhanced Oil Recovery, CNPC, Beijing, 100083, China*
[2]*Research Institute of Petroleum Exploration and Development, CNPC, Beijing 100083, China*
[3]*Polytechnic College, College of Engineering, Hebei Normal University, Shijiazhuang 050024, China*
E-mail: haokang@hebtu.edu.cn
[*]*Corresponding Author*

Received 16 August 2022; Accepted 20 September 2022;
Publication 31 January 2023

Abstract

With its abundant reserves in the world, carbonate reservoir has become one of the main targets for future oil and gas development. Accelerating the research and development of carbonate reservoirs is thus significant to enhance the world's energy supply capacity. However, there have been some problems in the evaluation of carbonate reservoirs for a long time, such as low description accuracy of fractured-vuggy bodies, diverse flow patterns, and difficult reservoir simulation and prediction. Compared with traditional manufacturing methods, 3D printing is an advanced manufacturing technology of rapid prototyping. It has the characteristics of short manufacturing cycle, not limited by the complexity of parts, material saving and energy saving, and thus has unparalleled advantages in reservoir rock analysis. In this paper, the carbonate core of Yingmaili region in Tarim Basin was taken as the research object, and the uniaxial compression mechanical properties of

Strategic Planning for Energy and the Environment, Vol. 42_2, 331–352.
doi: 10.13052/spee1048-5236.4224

three small cores printed with different materials were designed and tested by using KINGS-600 3D photocuring printer and photosensitive resin materials. After that, UV-9400S white resin with the highest strength is selected as the printing material of the full diameter core model of the karst cave. Combined with the CT scanning of the formed samples, the control accuracy concerning the cave morphology of the 3D printed samples was tested which adequately proves that flow experiments can be carried out with 3D printed core samples. At last, the article also analyzes the shortcomings of 3D printing technology, and points out the direction for its large-scale application in the field of oil and gas exploitation. This study can especially provide a reference for the application of 3D printing technology in the field of carbonate reservoir development, and ultimately promote the sustainable supply of oil and gas resources.

Keywords: Sustainable development, 3D printing, carbonate reservoir, flow patterns, reservoir characterization.

1 Introduction

In recent years, although human beings have made significant progress in the development of new energy [1–3], oil and gas resources still occupy a dominant position in the world's energy consumption. Despite the fact that many scholars have put forward new technologies that are conducive to sustainable development from their own professional point of view [4–6], whether underground oil and gas resources can be exploited continuously is still a major issue related to the sustainable development of human society [7–9]. Carbonate reservoirs have abundant reserves in the world, and have become the key areas for future hydrocarbon exploration and development. Accelerating the research and development in this field is of great significance to enhance the world's oil and gas supply capacity [10, 11]. In order to improve the recovery factor of carbonate reservoirs, many scholars have done a lot of research from different perspectives. Based on the exploration and development practice of Shunbei ultra-deep carbonate oil and gas field in Tarim Basin, Ma et al. systematically summarized the theoretical and technical progress of exploration and development during the "13th Five-Year Plan" period, providing reference and enlightenment for expanding the exploration field of this area and the exploration and development of ultra-deep marine carbonate around the world [12]. Based on the analysis of the characteristics of carbonate reservoirs in the Tarim Basin, Jiang et al.

proposed the geological theory and development technology of carbonate strike-slip fault-controlled reservoirs [13]. In view of the difficulty in predicting key development indexes of fractured-vuggy carbonate reservoirs, Chang et al. established a prediction method for key development indexes from a single reservoir to the whole block by using various methods, which can provide a basis for the preparation of development plans and the formulation of technical policies [14]. Yuan et al. proposed a set of systematic optimization process for development mode of fractured-vuggy carbonate reservoirs by means of numerical simulation, realizing the optimization of development mode of such reservoirs [15]. Sun et al. proposed a reservoir classification and evaluation method based on principal component biplot and K-means cluster diagram, which can provide certain technical support for determining the development mode of carbonate reservoirs in the Middle East [16]. Li et al. innovatively proposed a series of deep carbonate oil and gas development technologies after nearly 20 years of technical research and practice, aiming at the problems of low description accuracy, diverse flow modes and difficult simulation and prediction of carbonate fracture-cave bodies, and achieved good field implementation results [17]. According to the literature, the study of seepage mechanism can understand the flow characteristics of fluid in porous media and provide a basis for oilfield development and deployment decisions. This kind of study must be based on the analysis of reservoir rock properties. 3D printing technology is an advanced manufacturing technology of rapid prototyping, its essential principle is discrete and accumulation, that is, with the assistance of computer, through the slicing processing of solid model, the manufacturing of three-dimensional entity is transformed into the accumulation of two-dimensional level and the continuous superposition along the forming direction, and finally the manufacturing of three-dimensional entity is realized. Compared with traditional manufacturing methods, 3D printing has the characteristics of short manufacturing cycle, not limited by the complexity of parts, material saving and energy saving, and has unparalleled advantages in reservoir rock analysis [18]. In this paper, the carbonate core of Yingmaili in Tarim Basin is taken as the research object, and the KINGS-600 3D photocuring printer is used to print the full diameter core samples by selecting the photosensitive resin material with the best strength. Combined with the CT scanning of the formed sample, the control accuracy concerning the cave morphology of the 3D printed sample was tested, and it was proved that the sample could be effectively used for seepage experiment in the laboratory. The conclusion part of the article also analyzes the shortcomings of the sample and points out the direction for the wide application of 3D printing technology in the field of oil and gas exploitation.

2 Methodology

In this study of 3D printing, SLA technology is used, which is also called Stereo Lithography Appearance technology. In fact, SLA printing technology is adopted in the world's first printer, and its light source is ultraviolet light. SLA generally uses liquid photosensitive resins as printing materials: transparent materials, white photosensitive resins, high-toughness photosensitive resins, and translucent photosensitive resins. The printing principle of SLA is that liquid photosensitive resin is placed in a resin tank, and ultraviolet light irradiates the resin through a rapidly rotating mirror. After the resin is irradiated by ultraviolet light, it is quickly cured and formed. When the printing program is started, the lifting table is located at the height of one slice thickness below the liquid level. Furthermore, the focused laser beam, under the control of a computer, performs laser scanning along the liquid surface according to the profile of the cross section of the printed object. At this time, the area scanned by the laser is quickly solidified, and then the lifting platform is lowered by the thickness of one slice to carry out laser scanning solidification. In this way, a physical model is finally formed after being stacked layer by layer. The specific printing principle and process are shown in Figures 1 and 2.

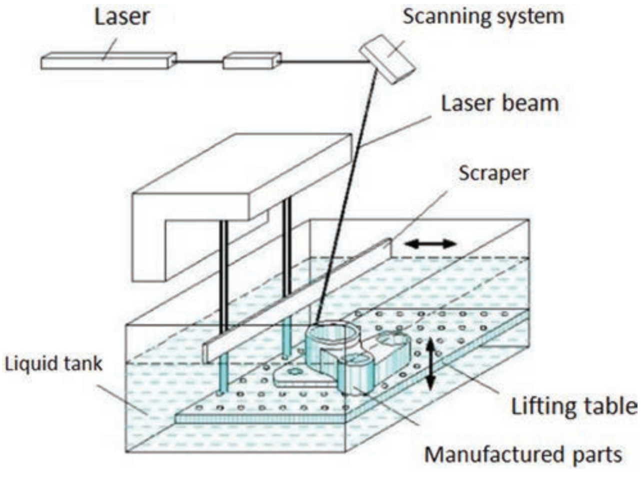

Figure 1 Principle of stereo lithography appearance 3D printing technology.

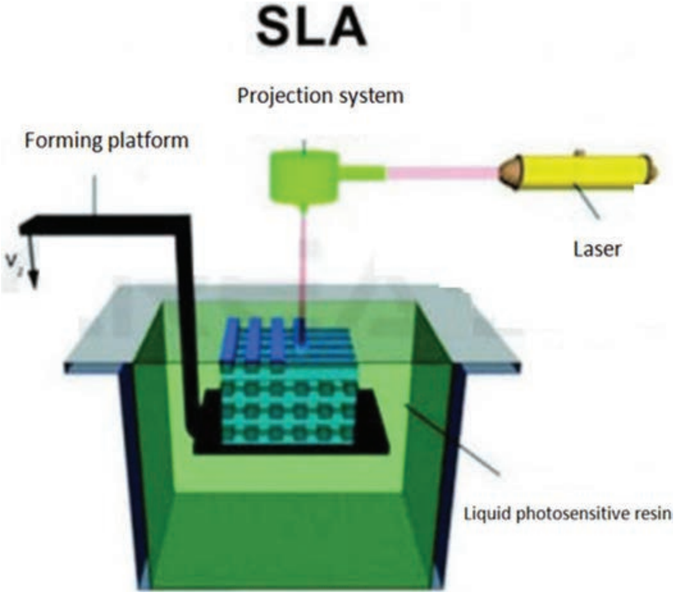

Figure 2 Technical process of stereo lithography appearance 3D printing technology.

3 Procedure of 3D Printing

3.1 Geological Conditions of Carbonate Fracture-cave Block in Yingmaili

The Ordovician carbonate rocks in Yingmaili block of Tarim Basin have extremely low matrix porosity and permeability, so their reservoir space are mainly structural fractures and secondary pores such as dissolution pores, caves and fractures. The spatial geometry is diverse, with great disparity in size and uneven distribution. According to the observation of core, imaging logging, cast thin section, scanning electron microscope and other data, the Ordovician carbonate reservoir space in the block can be divided into 3 categories and 12 sub-categories according to the geometry, size and genesis of the reservoir space [19–23]. The detailed classification can be see in Table 1 below [19–23].

3.2 Coarsening, Scaling and Extracting of 3D Geometrical Features of Karst Cave

Based on the needs on site, the geological characteristics and well group distribution of the carbonate fracture-cave block in Yingmaili block, YM2-12-5

Table 1 Ordovician carbonate reservoir space classification in Yingmaili

Morphological Classification	Genetic Classification	Diameter or Width (μm)	Geological Process
Karst cave	Giant cave	$>100 \times 10^3$	Dissolution
	Large cave	$10 \times 10^3 \sim 100 \times 10^3$	
	Medium cave	$5 \times 10^3 \sim 10 \times 10^3$	
	Small cave	$2 \times 10^3 \sim 5 \times 10^3$	
Fracture	Structural dissolution fracture	Of various sizes	Tectonization and dissolution
	Structural fracture	Below tens of microns	Tectonization and dissolution
	Pressure dissolution fracture	Below tens of microns	Diagenesis
Pore	Fracture pack hole	Tens to hundreds of microns	Filling
	Inter/Inner gravel pore	Tens to hundreds of microns	Weathering, tectonization and dissolution
	Matrix solution pore	Tens to hundreds of microns	Dissolution
	Inter-crystalline pore	Below tens of microns	Sedimentation and diagenesis
	Inner granular pore	Below tens of microns	Diagenesis

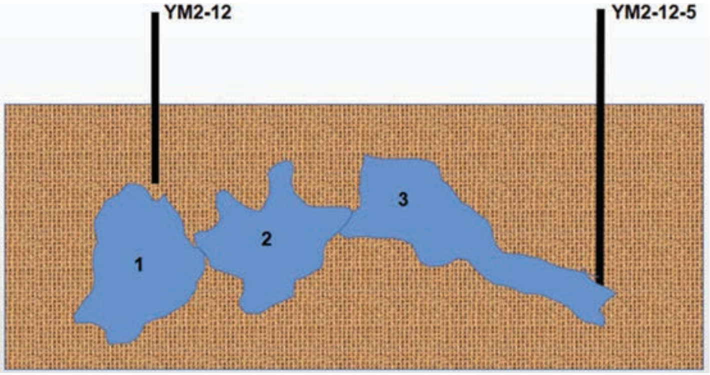

Figure 3 Pattern of well groups YM2-12-5 and YM2-12.

and YM2-12 well groups are selected as the research objects in this study. The distribution of main karst caves and the connection mode of well groups in this area are as shown in Figure 3. There are three typical karst caves in this area, which are numbered as 1, 2 and 3 respectively.

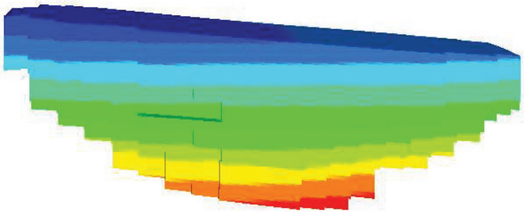

(a) Cave NO. 1

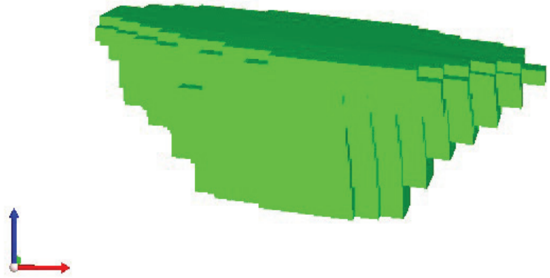

(b) Cave NO. 2

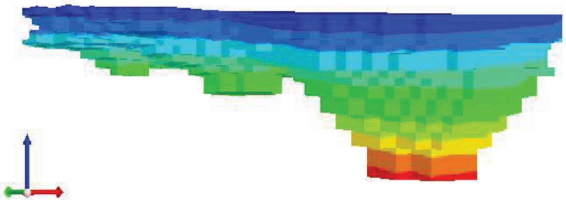

(c) Cave NO. 3

Figure 4 3D morphological view of the cave.

Specifically, the three-dimensional morphological view of NO. 1, NO. 2, and NO. 3 karst caves are as shown in Figure 4.

According to the principle of similar model design, the three caves are placed in the full diameter core with the diameter of 10 cm and different lengths in equal proportion. See Table 2 for the three-dimensional size, scaling ratio and scaled size of the original karst cave.

The schematic diagram of the position of the scaled model in the full-diameter core and the schematic diagram of the assembly of other seepage channels are shown in Figure 5.

Table 2 Geometrical similarity data of karst cave

Cave	Prototype Size/m			Scale by	Similar Model Size/cm			Length of Full
NO.1	Length	Width	Height	Width	Length	Width	Height	Diameter Core/cm
1	282.8	193.7	95.3	39.275	7.2	4.9	2.4	12
2	282.6	238.2	104.8	39.275	7.2	6.1	2.7	12
3	467.6	314.2	109.1	39.275	11.9	8.0	2.8	16

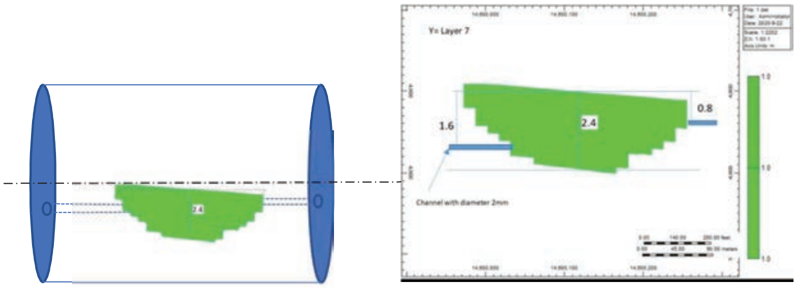

(a) Cave NO. 1

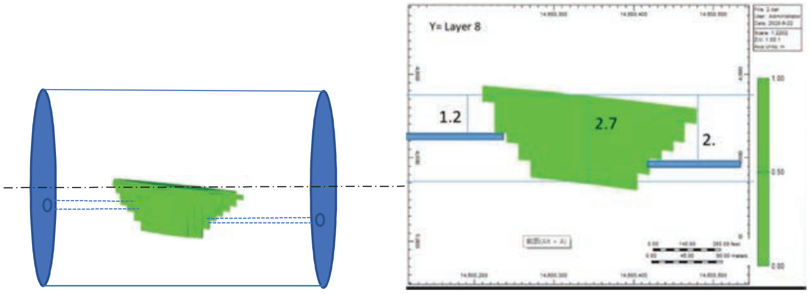

(b) Cave NO. 2

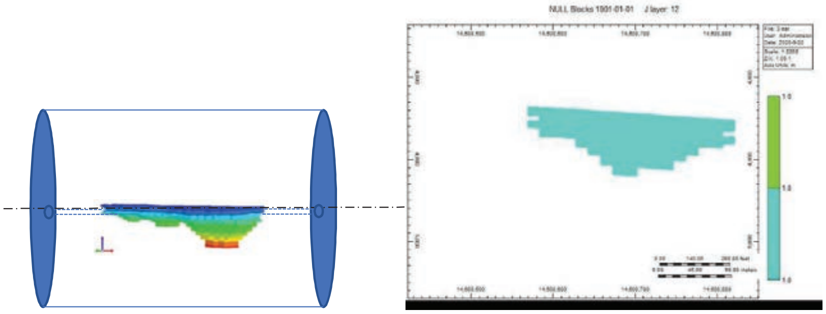

(c) Cave NO. 3

Figure 5 Assembly diagram of similarity model with karst cave after zooming.

3.3 Coarsening, Extraction and Reconstruction of Geometrical Model of Karst Cave

Interlayer thickness of karst cave is reduced by model coarsening, and YZ plan of karst cave is taken respectively. Among them, the No.1 karst cave is divided into 13 layers, with a single layer thickness of 14.9 m; the No.2 karst cave is divided into 16 layers, with a single layer thickness of 14.9 m; the No.3 karst caves are divided into 26 layers, with single layers thickness of 14.9 m.

The YZ section image of the cave is imported into ImageJ software for binarization. The image with multi-level gray values is replaced by binary pixels and converted into a binary image containing only two pixel distributions of 0 and 1. The key to obtain an ideal binary image is the selection of a reasonable segmentation threshold. Because the unreasonable selection of segmentation threshold can easily lead to unreasonable segmentation of the target object (that is, the background object is divided into target objects, or the target object is divided into background objects), thus affecting the accurate analysis of the structural characteristics of the target. The image segmentation threshold (T) can be defined as the gray threshold between the target object (segmented object) and the background object. Let F(i, j) denote the gray value of point (x, y) in the original image, the gray value of the target object in the segmented image is 1 and the background value is 0. After binarization, the gray value G (x, y) of the point (x, y) can be expressed as:

$$G(x,y) = \begin{cases} 1, & F(i,j) > T \\ 0, & F(i,j) < T \end{cases} \tag{1}$$

After binarization, the information of the gray image is stored in the pixel matrix composed of 0 and 1. The characteristics of pixels are only related to the spatial distribution of 0 and 1. Therefore, by retrieving the spatial position, number and connection relationship of pixels in the spatial matrix, the calculation of specific parameters, as well as the study of high-order image analysis and model extraction can be carried out (see Figure 6 for details).

Import the segmented image into Geomagic modeling software, and import the scaled thickness data of each layer. The model reconstruction algorithm is used to extract the geometric information of the cave in the image and reconstruct the geometric model of the cave. Then the corresponding geometric models of full diameter core and cylindrical seepage channel with diameter of 2 mm are established. Finally, the geometric assembly and

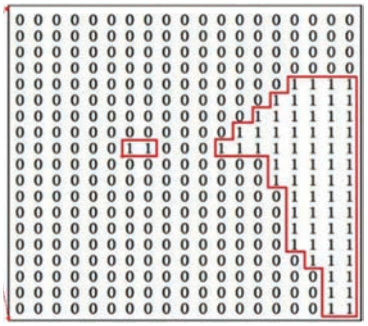

0	0	0	0	0	0	0	0	0	0	0	0	0	0	0	0	0	0	0
0	0	0	0	0	0	0	0	0	0	0	0	0	0	0	0	0	0	0
0	0	0	0	0	0	0	0	0	0	0	0	0	0	0	0	0	0	0
0	0	0	0	0	0	0	0	0	0	0	0	0	0	0	0	0	0	0
0	0	0	0	0	0	0	0	0	0	0	0	0	0	0	1	1	1	1
0	0	0	0	0	0	0	0	0	0	0	0	0	0	1	1	1	1	1
0	0	0	0	0	0	0	0	0	0	0	0	0	1	1	1	1	1	1
0	0	0	0	0	0	0	0	0	0	0	0	1	1	1	1	1	1	1
0	0	0	0	0	0	1	1	0	0	0	1	1	1	1	1	1	1	1
0	0	0	0	0	0	0	0	0	0	0	0	0	0	1	1	1	1	1
0	0	0	0	0	0	0	0	0	0	0	0	0	0	1	1	1	1	1
0	0	0	0	0	0	0	0	0	0	0	0	0	0	0	1	1	1	1
0	0	0	0	0	0	0	0	0	0	0	0	0	0	0	1	1	1	1
0	0	0	0	0	0	0	0	0	0	0	0	0	0	0	1	1	1	1
0	0	0	0	0	0	0	0	0	0	0	0	0	0	0	1	1	1	1
0	0	0	0	0	0	0	0	0	0	0	0	0	0	0	0	1	1	1
0	0	0	0	0	0	0	0	0	0	0	0	0	0	0	0	0	1	1
0	0	0	0	0	0	0	0	0	0	0	0	0	0	0	0	0	1	1
0	0	0	0	0	0	0	0	0	0	0	0	0	0	0	0	0	1	1

Figure 6 Numerical conversion of binary image.

Boolean operation of full-diameter core, seepage channel and karst cave model are realized, results are as shown in Figure 7.

3.4 Geometry Model Output of 3D Printing Core

Import the full diameter geometric model of the cave generated above into Material Magic software, and extract the 3D geometric model of the core solid range. Furthermore, the output parameters and accuracy are controlled and exported to the STL file format that can be recognized by the 3D printing device for storage. The KINGS-600 3D printer is used in this study. Based on SLA technology, photosensitive resin materials with different types and strengths are used as printing materials. The equipment is shown in Figure 8.

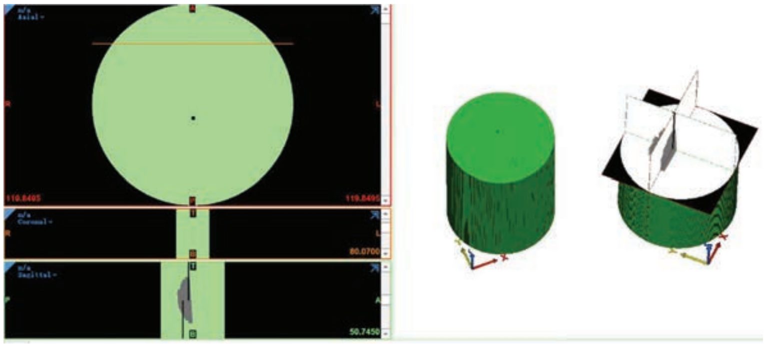

(a) Three-view drawing and sectional drawing of printed model for cave NO. 1

Figure 7 Continued

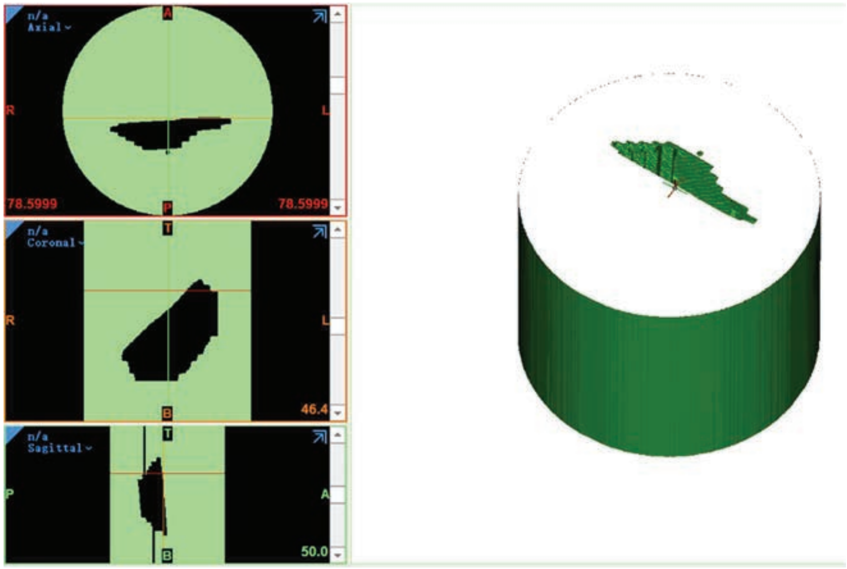

(b) Three-view drawing and sectional drawing of printed model for cave NO. 2

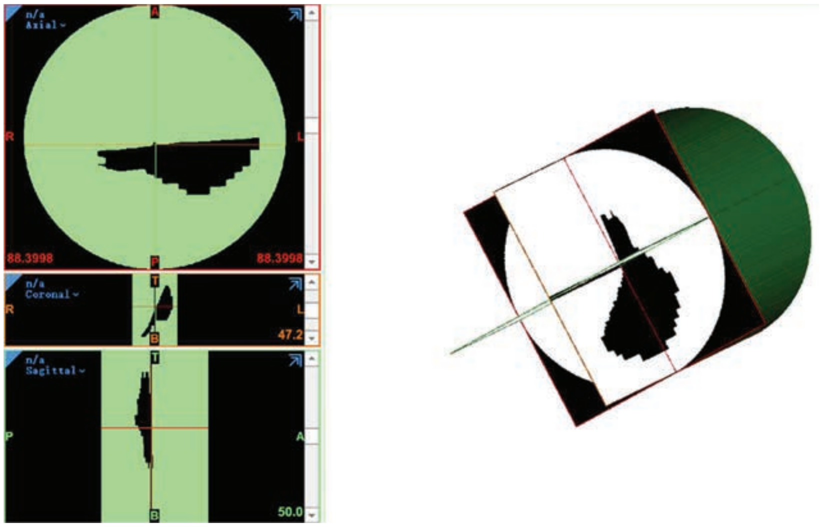

(c) Three-view drawing and sectional drawing of printed model for cave NO. 3

Figure 7 Geometrical model of full diameter core of karst cave with equal scaling.

Figure 8 KINGS-600 3D printer.

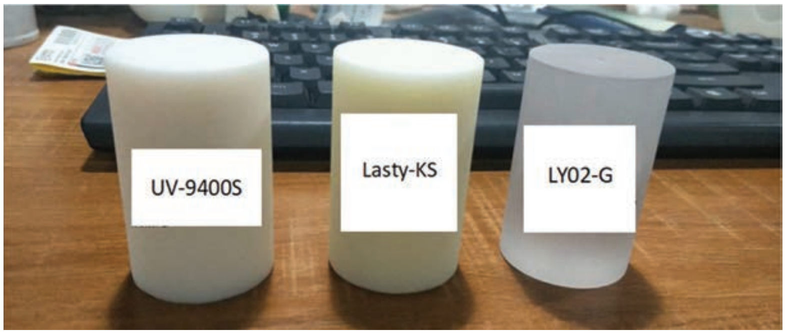

Figure 9 Appearance display of three resin materials.

4 Results and Discussion

4.1 Mechanical Strength Detection of 3D Printing Model Material

UV-9400S white resin, Lasty-KS yellow resin and LY02-G translucent resin were selected as the main photo-curing 3D printing materials. The appearance of the three materials is shown in Figure 9. In order to test the overall bearing capacity of the model after molding, this study first designed a simplified cave and seepage channel model: the cave is a sphere, and the upper and lower parts are a 5 mm cylindrical seepage channel connected with the core. The specific geometric configuration is shown in Figure 10.

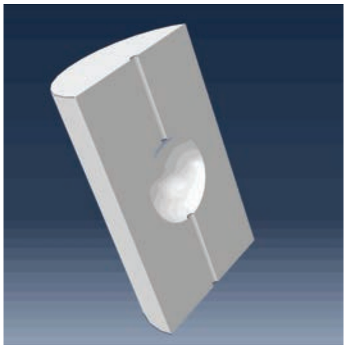

Figure 10 Simplified design of karst cave model.

Figure 11 Rock mechanics testing equipment—SHT-4106 material testing machine.

According to the specification of ASTM D7012-14e1, the uniaxial compression test of 3D printed rock was carried out by using the universal material testing machine SHT-4106 in the experimental center of the Civil Engineering Institute of Southwest Petroleum University, as shown in Figure 11. The maximum working load of the equipment is 1000 KN, and

Table 3 Mechanical properties of cave core sample

Sequence	Materials	Core Diameter (mm)	Core Length (mm)	Confining Pressure (MPa)	Elasticity Modulus (MPa)	Compressive Resistance (MPa)
1	White resin UV-9400S	25	60	0	1370.5	42.3
2	Yellow resin Lasty-KS	25	60	0	384.3	17.8
3	Translucent resin LY02-G	25	60	0	842.7	25.5

the measurement accuracy of force, displacement and deformation is 0.5%. In the experiment, the loading process was started by means of stress control, and the loading rate was 0.05 KN/s, until the sample is destroyed. Before carrying out the test, it is necessary to ensure that the end faces of the test sample are flat, and the error at both ends shall not be greater than 0.05 mm. The sample shall be placed in the center of the bearing plate in close contact with the compression head to ensure the uniform application of load and avoid the stress concentration effect at the end. Uniaxial compression test on the simplified karst cave core samples printed from the three materials is carry out after light curing, and the elastic modulus and compressive strength data of the core is obtained respectively, as shown in Table 3. It can be seen that the elastic modulus of the three types of cores are 1370.5 MPa, 384.3 MPa and 842.7 MPa respectively, which are lower than those of natural rocks. The uniaxial compressive strength of three kinds of core samples is 42.3 MPa, 17.8 MPa and 25.5 MPa. It is judged from test results that UV-9400S white resin has the best mechanical properties, so UV-9400S white resin is selected as the printing material for the carbonate fracture-cave model of Yingmaili block in this study.

4.2 3D Printing of Core and Morphological Detection of Karst Cave in it

The full-diameter core samples of white resin caves NO. 1, NO. 2 and NO. 3 obtained by 3D printing are shown in Figure 12. The cross-shaped position in the figure is the 2 mm diameter connecting channel of the cave inside the sample.

In order to determine the accuracy of the 3D printing sample and the angle of the installation direction of the experimental core, the printing sample is scanned by CT. The scanning equipment and process are shown in Figure 13. See Figures 14, 15 and 16 for the cave model and seepage channel model inside the core sample obtained by scanning. By comparing with the cave geometry extracted from the geological model, it is found that the cave shape

Figure 12 3D printing of full-diameter core samples of white resin with caves NO. 1, NO. 2 and NO. 3.

Figure 13 CT detection of 3D-printing full diameter cores.

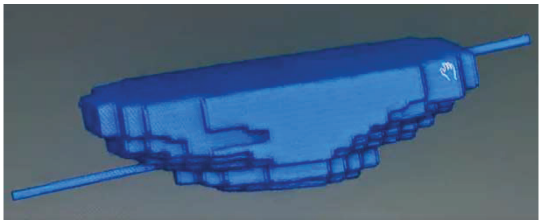

Figure 14 Reconstruction map of CT scanning results for NO.1 cave.

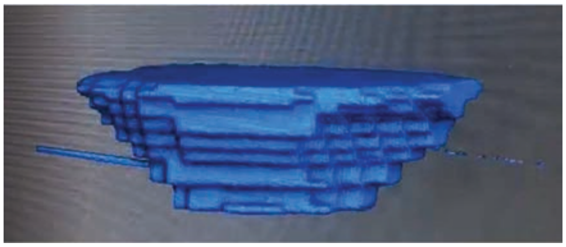

Figure 15 Reconstruction map of CT scanning results for NO.2 cave.

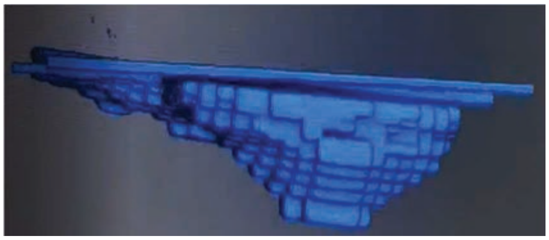

Figure 16 Reconstruction map of CT scanning results for NO.3 cave.

control of 3D printing core samples is in good agreement with the input parameters. According to the comprehensive judgment, 3D printing core samples can be used to carry out physical modelling experiments on seepage characteristics of complicated fractured-vuggy bodies in carbonate reservoir.

5 Conclusion

According to the field needs and the geological characteristics and well group distribution of the carbonate fracture-cave block in Yingmaili, YM2-12-5 and YM2-12 well groups are selected as the research object. Through the identification and extraction of the main large karst cave shapes in the three-dimensional geological model, combined with the technology of model coarsening, three small cores of different materials were printed by using the KINGS-600 3D light curing printer and photosensitive resin materials. After the inspection by mechanical test, UV-9400S white resin with the highest strength is selected as the printing material of the full diameter core model of the karst cave. Combined with the CT scanning of the formed sample, the control accuracy of the 3D printed sample was tested, and it was confirmed that the physical simulation experiment of seepage characteristics could be carried out based on the samples.

At the same time, the limitations of 3D printing technology should also be recognized. One of the biggest disadvantages of 3D printing resins for core flow experiments is that they have a limited range of strengths, which makes some experiments based on core strength impossible. Of course, this limitation has also been alleviated by certain technologies, such as researchers' 3D printing works is used as molds to create artificial rock structures with high-strength cement, which can capture complex surface geometries. Moreover, these artificial samples can be cast out of the mold indefinitely, thus obtaining consistent and repeatable test samples, which is conducive to obtaining more accurate research results.

Nevertheless, the application of 3D printing in the field of oil and gas has formed an established upward trend. In fact, the application of 3D printing technology in the field of oil and gas exploitation is far more than core analysis. In the field of oil and gas production, many equipment are operated under high pressure and harsh working conditions, and some process control components will inevitably fail. Keeping oil and gas production facilities running smoothly has been one of the toughest challenges in the industry. Considering the production and transportation cycle of components, in order not to delay production, oil and gas operators have to implement expensive inventory plans to avoid the risk of prolonged downtime. As a potential answer to such challenges, 3D printing has unique advantages in achieving more efficient and cost-effective solutions to address persistent inventory and geographical barriers.

Based on the reality, it is suggested that 3D printing technology can make efforts in the following aspects: First, enhance the research on 3D printing parameter development and component design to meet the challenges brought by the changing geometry and characteristics of printed components. These systems also require extensive redesign of the parts to make them printable, rather than allowing the parts to be printed the way they were originally designed. The second is to strengthen the research on the compatibility of printing files, so that the printing files set on one 3D printing device can be used directly on another machine of the same brand and model. This will reduce the amount of user intervention and avoid the challenges of digital inventory. Third, relevant associations, such as the American Petroleum Institute (API), should issue timely guidelines on the procurement or specifications of 3D printing materials on the basis of full investigation. This will help oil and gas companies to carry out specific applications of 3D printing technology in a timely manner.

Acknowledgments

This work was supported by Scientific Research and Technology Development Project of PetroChina Company Limited (GRANT NO.: 2019A-0911) and by Open Fund of State Key Laboratory of Enhanced Oil Recovery, CNPC (GRANT NO.: 2022-KFKT-29). I would also like to thank the editorial and reviewer panel for their input and comments.

Conflict of Interest

The authors all declare that they have no conflict of interests regarding the publication of this paper.

References

[1] Xueping Yang. 'Exploration on technical path of modern coal chemical industry under the background of carbon neutralization', Chemical Industry and Engineering Progress, vol. 41, no. 7, pp. 3402-3412, 2022.
[2] Yongchao Luan, Yalin Xiong, Guangli He, et al. 'Research progress of hydrogen separation membrane', Strategic Study of CAE, vol. 24, no. 3, pp. 140–152, 2022.
[3] Maoyuan Li, Yun Zhang, Zhengtang Wang, et al. 'Microstructure evolutions in lithium ion battery electrode manufacturing', Chinese Science Bulletin, vol. 67, no. 11, pp. 1088–1102, 2022.
[4] Ziwei Yan, Chunying Cui, Chenjia Liao. 'The impact of green finance on clean power generation: evidence based on China', Strategic Planning for Energy and the Environment, vol. 40, no. 4, pp. 421–436, 2021.
[5] Xiaotian Wang, Hui Zhao. 'Analysis and comparison of China's biofuel ethanol subsidy modes', Strategic Planning for Energy and the Environment, vol. 40, no. 4, pp. 363–386, 2021.

[6] Yadong Guo, Zhao Meina. 'Research on sustainable energy development from the perspective of focusing on carbon peaking and neutrality', Strategic Planning for Energy and the Environment, vol. 41, no. 3, pp. 345–362, 2022.

[7] Meifang Hou, Songqi Pan, Hanlin Liu. 'World energy trend and China's oil and gas sustainable development strategies', Natural Gas Industry, vol. 41, no. 12, pp. 9–16, 2021.

[8] Jian Su, Yingbo Liang, Lin Ding, et al. 'Research on China's energy development strategy under carbon neutrality', Bulletin of the Chinese Academy of Sciences, vol. 36, no. 9, pp. 1001–1009, 2021.

[9] Yu Yang, Ze He. 'China's overseas oil and gas dependence: situation, geographical risks, and countermeasures', Resources Science, vol. 42, no. 8, pp. 1614–1629, 2020.

[10] Kuanzhi Zhao, Lijuan Zhang, Duoming Zheng, et al. 'A reserve calculation method for fracture-cavity carbonate reservoirs in Tarim Basin, NW China', Petroleum Exploration and Development, vol. 42, no. 2, pp. 251–256, 2015.

[11] Weiyun Zhan, Haiyong Yi, Haitao Li, et al. 'Evaluation methods for the upgraded controllable and predicted reserves in carbonate gas reservoirs', Natural Gas Exploration and Development, vol. 45, no. 1, pp. 8–14, 2022.

[12] Yongsheng Ma, Xunyu Cai, Lu Yun, et al. 'Practice and theoretical and technical progress in exploration and development of Shunbei ultra-deep carbonate oil and gas field, Tarim Basin, NW China', Petroleum Exploration and Development, vol. 49, no. 1, pp. 1–17, 2022.

[13] Tongwen Jiang, Lunjie Chang, Xingliang Deng, et al. 'Geological understanding and evaluation technology of fault controlled carbonate reservoir development: A case study of the Tarim Basin', Natural Gas Industry, vol. 41, no. 3, pp. 1–9, 2021.

[14] Baohua Chang, Shiyin Li, Wen Cao, et al. 'Prediction method of key development indicators of fracture-cavity carbonate reservoirs and its application', Special Oil & Gas Reservoirs, vol. 28, no. 2, pp. 72–77, 2021.

[15] Shibao Yuan, Wenqiang Liu, Haiyan Jiang, et al. 'Investigation into development modes of fracture-cavity carbonate reservoirs based on reservoir characteristics', Petroleum Geology and Recovery Efficiency, vol. 28, no. 1, pp. 80–87, 2021.

[16] Liang Sun, Yong Li, Baozhu Li. ‘Classified evaluation methods and waterflood development strategies for carbonate reservoirs in the Middle East’, Acta Petrolei Sinica, vol. 43, no. 2, pp. 270–280, 2022.

[17] Yang Li, Zhijiang Kang, Zhaojie Xue, et al. ‘Deep carbonate oil and gas development technology fuels China’s petroleum industrial development’, Oil Forum, vol. 40, no. 3, pp. 33–42, 2021.

[18] Zhilin Li, Lei Li, Chun Wang, et al. ‘The 3D printing technology and the application research in petrochemical industry’, Guangdong Chemical Industry, vol. 41, no. 23, pp. 100–101, 2014.

[19] Xingxi Zhou. ‘A primary discussion on the network-like oil and gas pools in carbonate rocks- taking the Lunnan Ordovician buried-hill pool in Tarim basin as an example’, Petroleum Exploration and Development, vol. 27, no. 3, pp. 5–8, 2000.

[20] Wei Yang, Qinghua Wang, Deren Zhao, et al. ‘Fractures of Ordovician carbonate rocks in Hetian river gasfield’, Oil & Gas Geology, vol. 21, no. 3, pp. 252–255, 2000.

[21] Xiangbin Yan, Zhenhua Han, Yonghong Li. ‘Some cognition on characteristics of ordovician carbonate reservoirs in Tahe oil fields’, Marine Origin Petroleum Geology, vol. 6, no. 4, pp. 8–14, 2001.

[22] Kang Xu, Bingsong Yu, Sitong Liu. ‘Reservoir characteristics and main controlling factors of Yamaili region in Tarim basin’, Xinjiang Geology, vol. 31, no. 1, pp. 42–46, 2013.

[23] Haitao Zhao, Qi Sun, Wenhao Li, et al. ‘Cretaceous hydrocarbon accumulation rules of the Yingmaili area in the Tabei uplift: A case study of the Yingmai 46 well block’, Journal of China University of Mining & Technology, no. 1, pp. 137–147, 2022.

Biographies

Xu Chen received the bachelor's degree in Mechanical design, manufacturing and automation in 2010 and master's degree in Business Administration from China University of Petroleum in 2017. He is currently working at the Enhance Oil Recovery Center of Research Institute of Petroleum and Exploration Development. His research areas include petrophysics and enhance oil recovery.

Zubo Zhang received the bachelor's degree from Oil-Gas Field Development of Engineering Northeast Petroleum University in 1984. He is currently working at the Enhance Oil Recovery Center of Research Institute of Petroleum and Exploration Development. His research areas include petrophysics and enhance oil recovery.

Jian Gao received the bachelor's degree in Petroleum Engineering from Southwest Petroleum University in 1998, and the philosophy of doctorate degree in Petroleum and Natural Gas Engineering from China University of Petroleum in 2007, respectively. He is currently working at the Research Institute of Petroleum Exploration and Development, PetroChina. His research areas include exploitation and utilization of energy resources.

Hao Kang received the bachelor's degree in Petroleum Engineering from China University of Petroleum in 2008, and the philosophy of doctorate degree in Petroleum Geology from Peking University in 2014, respectively. He is currently working at the College of Engineering, Hebei Normal University. His research areas include exploitation and utilization of energy resources.